PCCP

Physical Chemistry Chemical Physics

www.rsc.org/pccp

Volume 10 | Number 15 | 21 April 2008 | Pages 1985–2124

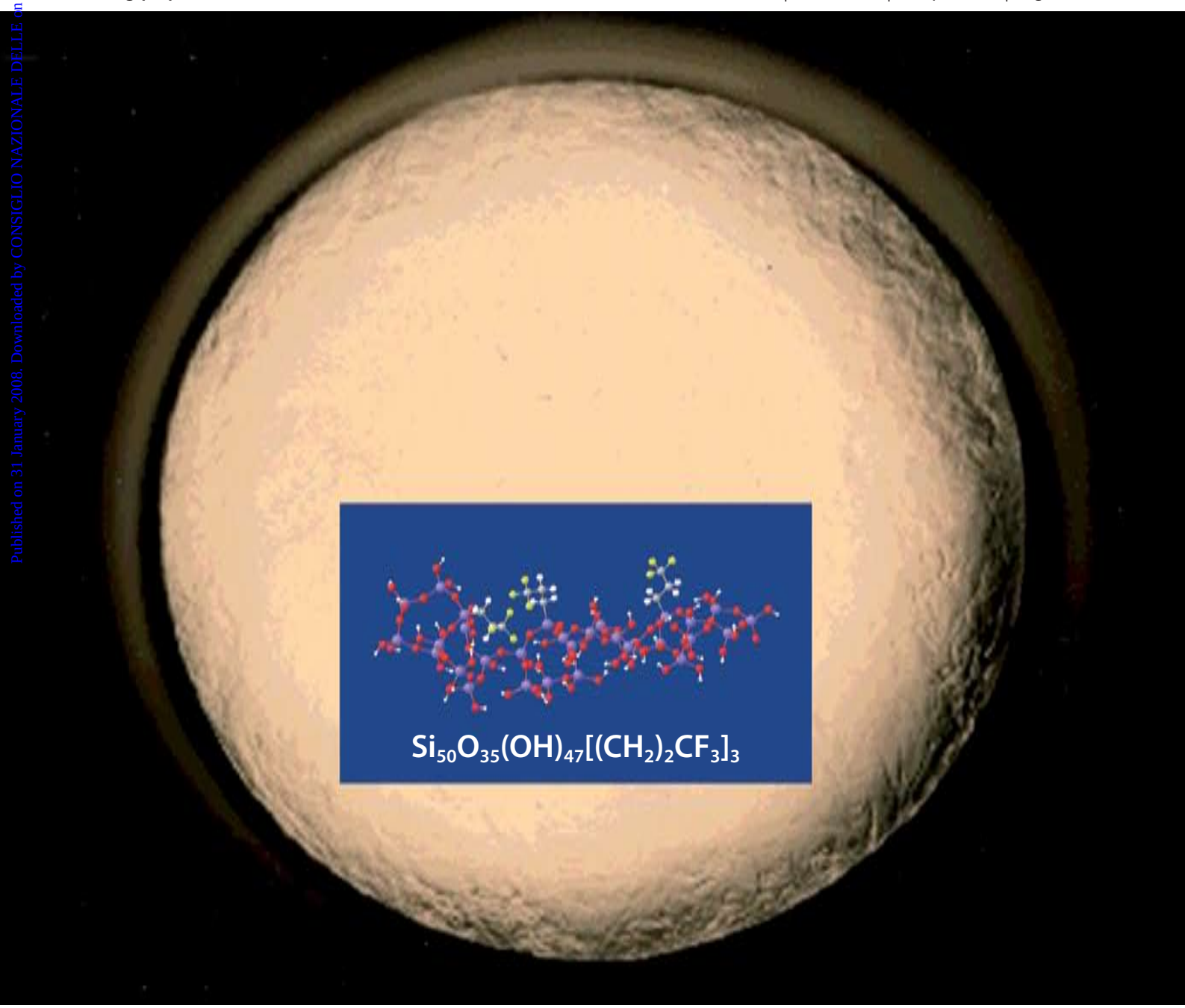

ISSN 1463-9076

The grounds for the activity of TPAP in oxidation catalysis in supercritical carbon dioxide when confined in hybrid fluorinated silica matrices

Alexandra Fidalgo,[a] Rosaria Ciriminna,[b] Laura M. Ilharco,*[a] Sandro Campestrini,[c] Massimo Carraro[c] and Mario Pagliaro*[b]

Received 24th October 2007, Accepted 19th December 2007
First published as an Advance Article on the web 31st January 2008
DOI: 10.1039/b716405j

Fluorinated organo-silica gels doped with tetra-*n*-propylammonium perruthenate (TPAP) are excellent catalysts for the aerobic oxidative dehydrogenation of alcohols in supercritical CO_2 ($scCO_2$). Their activity and stability are subtly dictated by structure, depending on the degree of fluorination and on the length of the fluoroalkyl chain linked to the silica network. Such dependence reflects the hydrophilic–hydrophobic balance (HHB) of the matrix, as evaluated by diffuse reflectance infrared Fourier transform (DRIFT) spectroscopy. The remarkable correlation between the materials' HHB and reactivity provides a finding of general validity for reaction-controlled mechanisms, which opens the route to the synthesis of second generation sol–gel entrapped catalysts for the production of fine chemicals in $scCO_2$.

1. Introduction

For alcohol oxidation reactions in microreactor systems operating in a continuous mode, the catalyst tetra-*n*-propylammonium perruthenate ($[N(CH_2CH_2CH_3)_4]^+[RuO_4]^-$), or TPAP, has been successfully supported on alumina.[1] However, for batch reactors, it has been proved that immobilization is beneficial, either in resins,[2] in mesoporous silicalite MCM-41[3] or in sol–gel matrices.[4] The advantages of the recently proposed sol–gel catalyst *FluoRuGel* (fluorinated Ru-doped gel: an organofluorosilica matrix physically doped with TPAP) for the aerobic oxidation of alcohols in supercritical CO_2 have been well documented.[5,6] These remarkable catalysts owe their enhanced efficiency and stability to the encapsulation of TPAP in fluorinated organic–inorganic silica matrices.

We have recently shown, by comparison between the reactivity of TPAP in homogeneous medium and encapsulated in *FluoRuGel*, that entrapment within the fluoroalkyl-modified sol–gel silica matrix favours a different kinetic behaviour, as a consequence of the improved catalytic performance of TPAP.[6] This may result from a modification on the chemical properties of the entrapped catalyst by the different nature of the sol–gel cage, similar to what happens with dopant molecules in sol–gel matrices modified by co-entrapped surfactants.[7] In fact, the highly polar $-CF_3$ groups, with the negative charge in the F atoms,[8] concentrate at the cages surfaces,[9] and attract preferentially the $N(CH_2CH_2CH_3)_4^+$ cations, leaving mutually isolated RuO_4^- anions.[6] These become more available to mediate the oxidative dehydrogenation of the alcohol substrate. Nevertheless, the confinement of the RuO_4^- ions guarantees the proximity with the large cations that mitigate the strong oxidation power of RuO_4^- alone, thus promoting selectivity.[10]

In organically modified non-fluorinated matrices, kinetic studies have shown that alcohol oxidation reactions in $scCO_2$ are diffusion-controlled.[11] If this were the case in *FluoRuGel*, a higher degree of fluorination should enhance the catalytic activity of entrapped TPAP. However, by increasing the length of the modifying fluorinated alkyl chain or its content, a decrease in the catalyst activity was observed.[5] The grounds for this behaviour may further be related to the structure of the fluorinated matrix itself.

In previous works, the superior performance of entrapped catalysts in non-fluorinated ORMOSILs (organically modified silicates) has been correlated with structural characteristics of the matrix, assessed from the vibrational spectra and complementary characterization techniques.[12–14]

In the present work, two fluoroalkylated precursors, 3,3,3-trifluoropropyltrimethoxysilane (TFPTMOS) and 3,3,4,4,5,5,-6,6,7,7,8,8,8-tridecaoctafluorotriethoxysilane (TDOFTEOS), were used as modifiers in a tetramethoxysilane (TMOS) based silica network, in different contents. The model structures of the two fluorinated precursors are shown in Scheme 1. For simplicity, they will be referred as C_3F_3 and C_8F_{13}, respectively, from now on.

2. Experimental

2.1 Catalysts preparation

Several fluorinated xerogels were prepared by sol–gel processing a fluoroalkyl containing monomer (3,3,3-trifluoropropyltrimethoxysilane, TFPTMOS purchased from Fluka; or 3,3,4,4,5,5,6,6,7,7,8,8,8-tridecaoctafluorotriethoxysilane, TDOFTEOS purchased from ABCR GmbH & Co.,

[a] *Centro de Química-Física Molecular, Instituto Superior Técnico, Complexo I, Av. Rovisco Pais 1, 1049-001 Lisboa, Portugal. E-mail: lilharco@ist.utl.pt*
[b] *Istituto per lo Studio dei Materiali Nanostrutturati, CNR, via U. La Malfa 153, 90146 Palermo, ItalyE-mail: mario.pagliaro@ismn.cnr.it*
[c] *Dipartimento di Scienze Chimiche, Università degli Studi, via Marzolo 1, 35131 Padova, Italy*

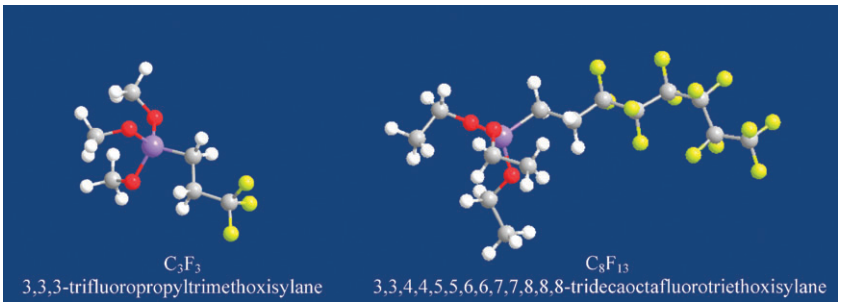

Scheme 1 Ball and stick models of the two fluoroalkylated precursors used in the synthesis of the *FluoRuGels*: -Si atom; -O atom; -C atom; -F atom; -H atom.

Karlsruhe) with tetramethoxysilane (TMOS) in the presence of TPAP dissolved in methanol (MeOH), and keeping constant the Si : MeOH : H_2O molar ratio at 1 : 8 : 4. Other chemicals, including benzyl alcohol, *n*-decane, MeOH, TMOS and TPAP were purchased from Sigma Aldrich and were used without further purification. Ultra pure water (Millipore Type 1) was used in all the preparations.

C_3F_3 series. A typical 10% trifluoropropyl doped silica gel, C_3F_3-10, was synthesised by adding TMOS (2.68 mL) and TFPTMOS (0.39 mL) to a solution of TPAP (24.5 mg) in MeOH (6.45 mL) cooled in an ice bath, followed by the addition of H_2O (1.44 mL). The mixture was stirred for 30 min, when it gelled yielding a black alcogel, which was sealed and left to age at room temperature for 24 h, prior to drying at 50 °C (5 days). The grey xerogel thus obtained was powdered, washed under reflux (CH_2Cl_2 × 2, 40 °C) and dried to 50 °C prior to use.

C_8F_{13} series. A typical 25% tridecaoctafluoro doped silica gel, C_8F_{13}-25 was synthesised, as mentioned above, by mixing TMOS (2.63 mL) and TDOFTEOS (1.12 mL) along with a solution of TPAP (21.3 mg) in MeOH (5.67 mL), followed by the addition of H_2O (1.42 mL). The resulting alcogel was treated as described above for C_3F_3-10, yielding a grey powder with a typical 0.022 mmol g^{-1} catalytic load. For sample C_8F_{13}-50, tetra-*n*-butylammonium fluoride (TBAF) was used as the catalyst for the sol–gel polycondensation.

2.2 Characterization of *FluoRuGels*

The porosity parameters of the fluorinated ORMOSILs were obtained from the analysis of N_2 adsorption–desorption isotherms at 77 K, performed with a Carlo Erba Instruments Sorptomatic 1900 powder analyser. The ruthenium contents of the catalysts were measured by inductively coupled plasma mass spectrometry (ICP-MS) with a HP 4500 spectrometer. The molecular structure of the *FluoRuGels* was analysed by diffuse reflectance infrared Fourier transform (DRIFT) spectroscopy, using a Mattson RS1 FTIR spectrometer with a Specac selector, in the range 4000 to 400 cm^{-1} (wide band MCT detector), at 4 cm^{-1} resolution. The catalytic oxidation procedure at 75 °C and 22 MPa and the analysis of reaction rates have been described in detail elsewhere.[6]

3. Results and discussion

Table 1 summarizes the activity for the oxidation of benzyl alcohol in $scCO_2$ and some physical properties (specific surface area, A_{BET}, and pore volume, V_p) of the *FluoRuGels* prepared with different contents of the two fluoroalkylated precursors (C_3F_3 and C_8F_{13} stand for the number of carbon and fluorine atoms in the alkyl chain; whereas the subsequent number refers to the degree of fluoroalkylation in molar percentage). Also included is the expected fluorine content, $F_{\%}$, estimated as the number of F atoms in each fluorinated alkyl chain multiplied by the molar percent of the fluoroalkylsilane (relative to the total Si precursors).

General trends can be drawn from the results in Table 1: an increase of the expected degree of fluorination results in a decrease of the matrix specific surface area, suggesting that a pore blocking effect by the fluorinated alkyl chains may occur; this decrease in A_{BET} is accompanied by a decrease in the specific pore volume, but the values obtained for the two precursors do not match.

The variations of A_{BET} and V_p with $F_{\%}$ (Fig. 1) clearly show that the samples with C_3F_3 and C_8F_{13} represent two independent families. When C_8F_{13} is the co-precursor (exception made for C_8F_{13}-50), the matrix has comparatively lower specific

Table 1 Expected fluorine content ($F_{\%}$), activity (k_{cat}) and textural properties (specific surface area, A_{BET}, and pore volume, V_p) of the *FluoRuGels* doped with TPAP. C_xF_y-*z* stands for *z*% modified gel with a fluoroalkylated chain containing *x* C atoms and *y* F atoms

Catalyst	TMOS (%)	$F_{\%}$ (%)	k_{cat}[a] × 10^3/mol^{-1} min^{-1}	A_{BET}/m^2 g^{-1}	V_p/cm^3 g^{-1}
C_3F_3-10	90	0.3	4.90	691	0.53
C_3F_3-25	75	0.8	2.14	657	0.42
C_3F_3-50	50	1.5	2.90	458	0.31
C_8F_{13}-10	90	1.3	1.82	308	0.70
C_8F_{13}-25	75	3.2	2.07	182	0.59
C_8F_{13}-50	50	6.5	1.42	12	0.05

[a] Reaction conditions: 0.5 mmol benzyl alcohol, 0.1 equiv. entrapped TPAP (156 mg for C_3F_3-25), V(vessel) = 10 mL, P = 22 MPa, T = 75 °C, O_2 (1 bar).

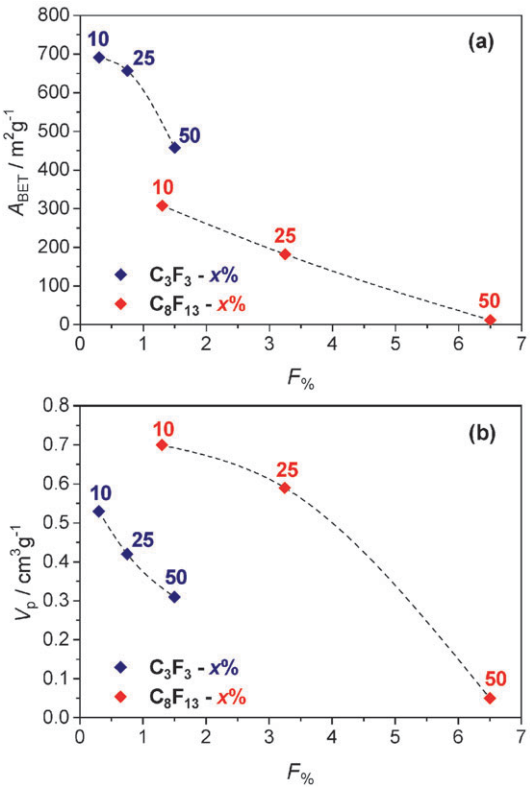

Fig. 1 (a) Specific surface area (A_{BET}) and (b) pore volume (V_p) as a function of the expected fluorine content of the *FluoRuGels* prepared with different contents (10 to 50 molar percent) of fluorinated precursor.

surface areas and higher specific pore volumes, suggesting that the pore morphology depends on the fluorinated precursor: the longer fluoroalkyl chain has higher flexibility and may act as a spacer, inducing larger pores in the network. The apparently low porosity of the sample C_8F_{13}-50 has been previously associated with the use of TBAF as a polycondensation catalyst.[5]

On the other hand, the results in Table 1 show that the catalyst's activity does not follow a systematic trend with the expected fluorine content or the textural properties. Its variation may rather be the result of structural differences in the matrices. These were analyzed from the DRIFT spectra shown in Fig. 2, which were normalised to the maximum of the ν_{as}SiOSi band. The main spectral regions are indicated.

Some striking features of the spectra deserve a comment. The broad OH stretching band (3700–2800 cm^{-1}) is assigned to uncondensed silanol groups and to adsorbed water. From the HOH deformation band ($\sim$1650 cm^{-1}), it becomes clear that the matrices with C_8F_{13} have negligible quantities of water, whereas those with C_3F_3 are able to adsorb small amounts. Since adsorbed water is hydrogen bonded to the network, the frequency of the νOH mode is expected to appear downshifted.[15]

In the spectra of Fig. 2a, this band not only shifts to higher wavenumbers as the fluorination content increases, but decreases in relative intensity. Apparently, the OH groups become increasingly free of interactions and their relative amount decreases with increasing fluorination. Furthermore, a νOH component at $\sim$3670 cm^{-1} that is assigned to free OH

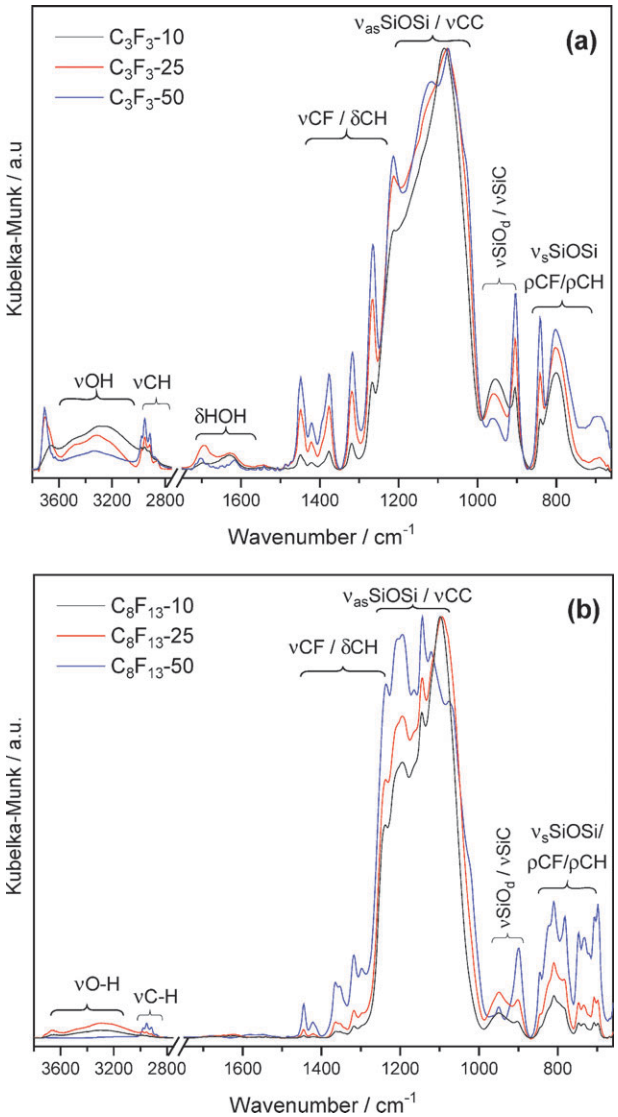

Fig. 2 DRIFT spectra of the *FluoRuGels*, normalized to the maximum of the ν_{as}SiOSi band: (a) C_3F_3; (b) C_8F_{13}.

groups increases with the fluorination content.[16] Globally, the relative intensity of the νOH band decreases, which is perfectly compatible with growing hydrophobicity of the matrices. In Fig. 2b, the absence of the adsorbed water fingerprint leads to assigning the νOH band exclusively to unreacted silanol (Si–OH) groups. In both series, the relative intensities of the bands related to CF and CH vibrational modes increase with increasing content of the fluorinated precursor.

For a more detailed analysis, the normalization to the maximum intensity of the spectra is not a correct procedure, since the ν_{as}SiOSi band is much distorted by CC, CH_2 and CF_2 related modes in the C_8F_{13} series. Instead, the spectra were decomposed in four regions: 4000–2600 cm^{-1}, 2100–1350 cm^{-1}, 1350–850 cm^{-1}, and 850–650 cm^{-1}. This decomposition into Gaussian and Lorentzian components followed a non-linear least squares fitting method, the positions of the components in each spectral region being previously determined by analysis of the second derivative of the spectra. The results are summarized in Table 2.

Table 2 Assignments of the DRIFT spectra of the *FluoRuGels* based on the spectral decompositions: wavenumber ($\tilde{\nu}$) in cm^{-1} and area (A) in %

C_3F_3-10		C_3F_3-25		C_3F_3-50		C_8F_{13}-10		C_8F_{13}-25		C_8F_{13}-50		
$\tilde{\nu}$	A	$\tilde{\nu}$	A	$\tilde{\nu}$	A	$\tilde{\nu}$	A	$\tilde{\nu}$	A	$\tilde{\nu}$	A	Assignments[15,16,19]
3668	1.5	3673	3.1	3669	2.8	3658	0.3	3662	0.7			νOH_{free}
3539	2.7	3476	4.3	3507	1.8	3518	0.5	3523	0.8			νOH
3323	8.3	3307	3.7	3315	3.0	3321	2.2	3319	3.6	3291	0.1	
3153	9.2	3173	2.5	3119	1.4	3182	1.9	3138	2.4	3141	0.2	
2982	0.1	2981	0.2	2982	0.5	2985	0.05	2985	0.1	2980	0.3	$\nu_{as}(C)CH_2$
2953	0.3	2954	1.1	2953	1.6	2952	0.04	2952	0.1	2952	0.4	$\nu_s(C)CH_2$
2919	0.3	2918	0.7	2916	0.7	2914	0.03	2916	0.1	2918	0.3	$\nu_{as}(Si)CH_2$
2871	0.1	2874	0.3	2871	0.6					2876	0.1	$\nu_s(Si)CH_2$
1690	0.3	1694	0.6	1700	0.2					1682	0.1	δHOH
1631	0.6	1629	1.0	1620	0.2	1643	0.2	1637	0.3			
1543	0.1	1549	0.1			1539	0.05	1545	0.04	1565	0.2	$\delta HOH_{chem.}$
1448	0.3	1448	1.0	1448	1.9	1445	0.04	1445	0.1	1445	0.5	$\nu_{as}CF_3$
1420	0.1	1420	0.4	1420	0.7	1420	0.05	1420	0.1	1420	0.3	δCH_2
1388	0.1	1388	0.4	1389	0.9							δCH_2
1376	0.3	1376	0.7	1376	1.4	1363	0.1	1366	0.1	1365	0.5	ν_sCF_3
						1347	0.14	1354	0.2	1352	0.8	$\nu_{as}CF_2$
1319	0.5	1318	1.0	1317	1.7			1318	0.4	1318	1.4	τCH_2
						1304	0.2	1298	0.31	1298	0.4	ν_sCF_2
1269	1.3	1267	3.4	1266	5.5	1245	6.4	1245	6.6	1243	11.4	τCH_2
1223	5.1	1227	2.0	1224	2.0	1216	11.3	1220	8.0	1222	2.5	$\nu_{as}SiOSi(LO_6)$
1217	0.1	1211	4.4	1212	5.6	1212	0.3	1212	0.7	1211	4.0	$\omega(Si)CH_2$
						1192	1.9	1193	2.6	1191	4.4	δCF_2
1158	27.0	1161	25.0	1168	17.8	1164	24.3	1165	24.0	1170	21.0	$\nu_{as}SiOSi(LO_4)$
1139	0.5	1134	1.3	1140	2.2	1146	1.0	1145	1.6	1144	1.9	νCC
1124	0.3	1119	0.8	1120	2.6	1121	0.8	1121	1.1	1121	3.0	νCC
1080	22.2	1077	21.2	1078	26.1	1096	33.8	1090	28.1	1087	22.0	$\nu_{as}SiOSi(TO_4)$
		1075	0.1	1074	0.8	1064	0.3	1065	0.3	1066	2.2	νCC
1036	6.2	1034	5.7	1036	3.7	1055	6.6	1047	5.6	1039	2.7	$\nu_{as}SiOSi(TO_6)$
1022	0.3	1021	1.2	1021	2.8	1018	0.8	1017	1.7	1018	2.1	ωCH_2
962	3.1	960	2.4	962	0.8	947	1.94	947	2.5	950	0.58	νSiO_d[a]
928	2.4	924	1.1	938	0.8							
904	1.02	904	2.09	904	2.76	901	0.46	901	1.11	901	2.40	ρCH_2
842	0.4	842	0.9	841	0.9	847	0.1	847	0.2	846	0.6	νSiC
819	1.5	813	0.9	807	0.3	824	0.9	825	1.2	827	1.5	ρCH_2
						810	0.4	810	0.5	809	1.5	ρCF_2
793	3.1	794	4.8	791	3.3	795	1.3	796	1.9	796	2.4	ν_sSiOSi
						781	0.3	780	0.6	781	1.4	ρCF_2
						748	0.2	748	0.4	748	1.2	$\rho(C)CH_2$
730	0.16	730	0.2	731	0.4	733	0.5	733	0.6	732	1.6	$\rho(Si)CH_2$
								719	0.04	719	0.1	ρCF_2
						708	0.3	708	0.6	708	1.3	ρCF_2
692	0.04	693	0.3	697	0.8	697	0.2	698	0.4	697	1.9	ρCF_3

[a] Dangling oxygen atoms, including Si–OH and $Si–O^-$.[17]

The components' assignments took into account not only the wavenumber but other considerations, such as the existence of CF_2 groups exclusively in the C_8F_{13} series. For each *FluoRuGel* family, the percent areas of the bands were estimated with respect to the fully integrated spectrum, thus overcoming the fact that all the bands vary with the precursor's content. The relative areas of similar bands will be analysed separately for the two series, since there are bands related to different groups, with different absortivities and differently coupled.

In the fingerprint region of the silica network ($\nu_{as}SiOSi$ band), the predominance of two types of primary siloxane rings [$(SiO)_4$ and $(SiO)_6$] was taken into account.[18] Their splitting into a pair of longitudinal-optic (LO)/transverse-optic (TO) components resulted in the assignments indicated in Table 2: $\nu_{as}SiOSi(LO_6)$ at $\sim$1220 cm^{-1}, $\nu_{as}SiOSi(LO_4)$ at $\sim$1160 cm^{-1}, $\nu_{as}SiOSi(TO_4)$ at $\sim$1080 cm^{-1}, and $\nu_{as}SiOSi(TO_6)$ at $\sim$1040 cm^{-1}.[19] The percentage of $(SiO)_6$ rings in the silica network ($\%Q_6$) was estimated by the ratio: $[A(LO_6) + A(TO_6)]/[A(LO_6) + A(TO_6) + A(LO_4) + A(TO_4)]$. For each series of *FluoRuGel*, the value of $\%Q_6$ decreases as the expected fluorine content increases, but the structure of the fluorinated precursor will certainly influence the trend. For equivalent compositions, the longer C_8F_{13} chains are expected to induce a higher percentage of the larger, less strained 6-rings (with the usual exception of sample C_8F_{13}-50), thus contributing to higher total pore volumes. If this assumption were correct, then the structural characteristic $\%Q_6$ must relate with the total pore volume (V_p) of the matrix, independently of the precursor series.[20] The correlation is shown in Fig. 3.

Since none of the DRIFT spectra shows features assignable to CH_3 groups, we may conclude that (i) either both co-precursors underwent full hydrolysis, (ii) or only TMOS was fully hydrolysed, the non-hydrolysed fluoroalkyl precursor being leached by the washing process. In contrast, condensation was not complete in any matrix, as all of them contain residual silanol groups. Since the νOH band may include water

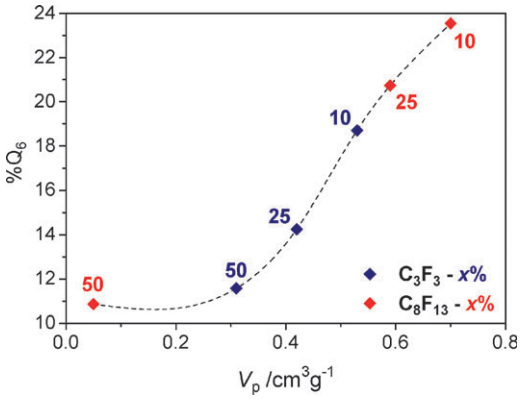

Fig. 3 Correlation of the structural parameter $\%Q_6$ with the total pore volume of the fluoroalkylated matrices prepared with 10 to 50 molar percent of fluorinated precursors.

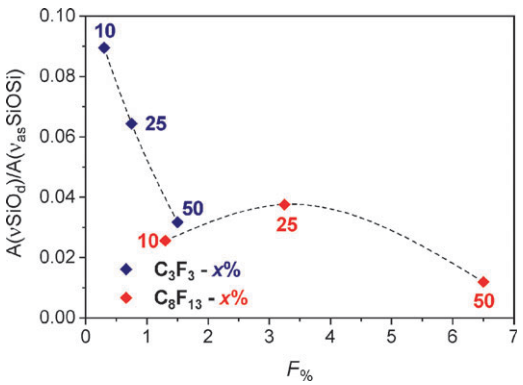

Fig. 4 Efficiency of condensation as a function of the expected fluorine content for *FluoRuGels* prepared with 10 to 50 molar percent of fluorinated precursors.

contributions, especially in the case of the C_3F_3 matrices, a measure of the condensation efficiency may be obtained from the relative intensity of the dangling Si–O stretching mode with respect to the condensed silica fingerprint: $[A(\nu SiO_d)/A(\nu_{as}SiOSi)]$. The dependence of this ratio on the expected degree of fluorination is shown in Fig. 4.

For the C_3F_3, series, it is very clear that the condensation yield increases with the degree of fluorination. This may be viewed as a consequence of the increasing hydrophobic interactions between the fluorinated chains, which bring about a close proximity of the reactive Si–OH groups. In the C_8F_{13} series, the hydrophobic interactions between the long fluorinated chains may rather induce "micelle-like" aggregates, with the opposite effect of taking apart the silanol groups. Therefore, a decrease in the condensation yield would be expected with increasing fluorine content. The anomalous result for C_8F_{13}-50 is due to the use of TBAF as an additional condensation catalyst for this sample.

With the purpose of testing the above assumptions, possible *FluoRuGel* structures obtained for samples C_3F_3-10 and C_8F_{13}-10 were optimised by energy minimization with Chem3D Ultra 9.0 (MOPAC module). The results are shown in Scheme 2.

Although the number of structural units used in these models is small (three fluoroalkylated precursor units in each case), the flexibility of the long tridecaoctafluoro chains is quite evident, as well as their tendency to aggregate due to strong hydrophobic interactions. Imagine the effect of increasing the content of fluorinated precursor!

The stretching modes of the CF_3 groups are excellent to follow the evolution of the fluorine content in each series, because each fluorinated precursor has only one such group. This is well rendered by Fig. 5, where the relative intensity of those modes, $\%CF_3$, estimated as $[A(\nu_{as}CF_3) + A(\nu_sCF_3)]$, is represented as a function of the expected fluorine content.

Predictably, the two trends converge in the axis origin, leaving out the C_8F_{13}-50 matrix, whose $\%CF_3$ suggests a much higher fluorination than expected. This probably results from a reduced leaching (upon washing) of the hydrolysed fluorinated precursor, whose co-condensation with the inorganic precursor was promoted by the presence of TBAF.

On the whole, if a reaction in a porous matrix is diffusion-controlled, the determining parameters will be the porosity and the solvent-matrix interactions. Accordingly, reactions in $scCO_2$ should be favoured by high lipophilicity and low hydrophilicity of the matrix, *i.e.*, low HLB values. This is the usual case in non-fluorinated matrices.[14] In fluorinated systems, one could argue that a more appropriate parameter to judge the matrix–solvent interactions would be the hydrophilic–hydrophobic balance (HHB) of the matrix. The increase in the matrix fluorine content would result in an increase in the catalyst activity (due to a decrease in the matrix HHB), followed by a decrease (when the pore blocking effect becomes prevailing). The fluorine content corresponding to the maximum activity would depend on the chain length.

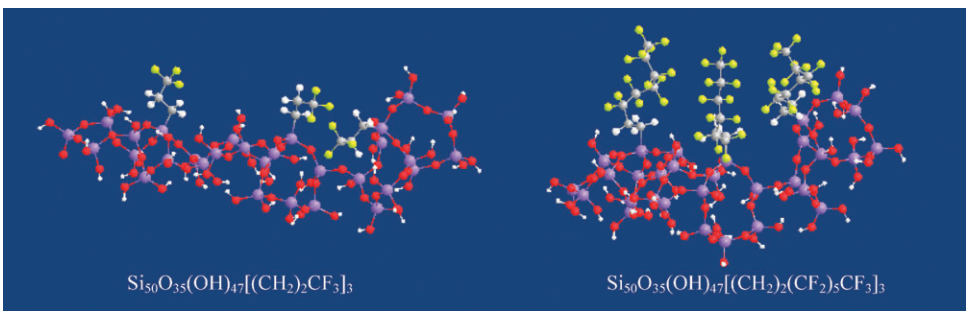

Scheme 2 Models of possible structures of *FluoRuGels* prepared with 90% TMOS and 10% C_3F_3 or C_8F_{13}. MOPAC energy minimisation for $Si_{30}O_{59}(OH)_{47}(Fluoroalkyl)_3$ formulations.

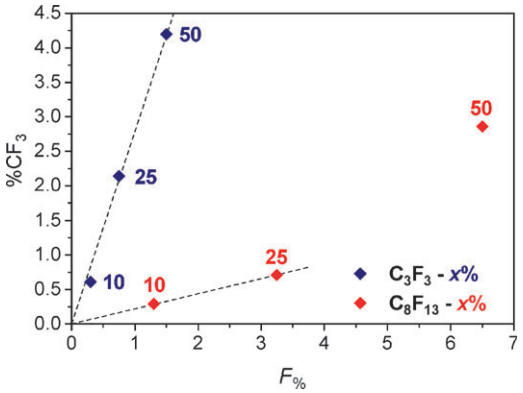

Fig. 5 Relative intensity of the νCF_3 modes as a function of the expected fluorine content for *FluoRuGels* prepared with 10 to 50% of fluorinated precursors.

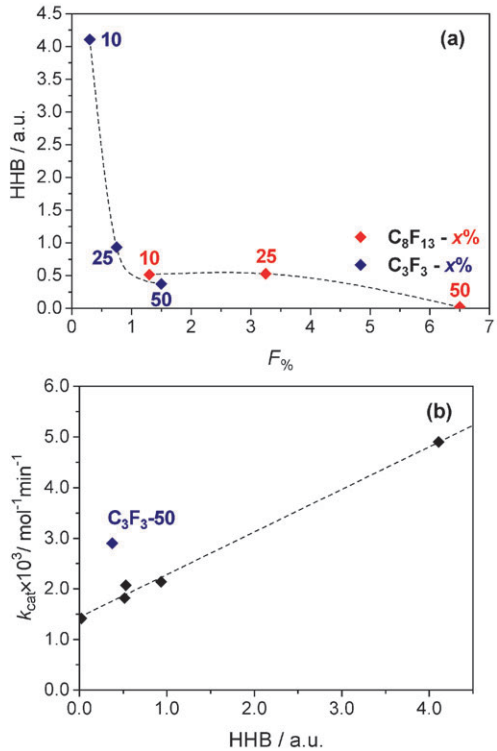

Fig. 6 *FluoRuGels* prepared with 10 to 50% of fluorinated precursors (a) HHB of the matrices as a function of the fluorine content; (b) activity of TPAP as a function of HHB.

On the other hand, for reactions in $scCO_2$ within hydrophobic matrices, diffusion must be a very fast process and the reaction becomes the controlling step. In this case, the determining interactions are reagents-matrix, assuming that the catalyst is accessible, at the pores' surface.[5] The reagents being polar, activity should increase with increasing HHB, except if a pore blocking effect shifts the process to diffusion-controlled.

The HHB of the *FluoRuGels* was estimated by ratioing %OH [$A(\nu OH) + A(\nu Si–O_d)$] against %CF [$\sum A(\nu CF) + \sum A(\delta CF) + \sum A(\rho CF)$]. The variation of the HHB thus obtained with the expected fluorine content is shown in Fig. 6a. The dependence of the activity of encapsulated TPAP on HHB is depicted in Fig. 6b.

Independently from the fluoroalkylated precursor, we may conclude that the HHB is a true structural parameter, since it decreases consistently with the expected fluorine content. The variation of TPAP activity with the matrix HHB clearly shows that the aerobic oxidation of benzyl alcohol in these *FluoRuGels* is a reaction-controlled process. Exception is made for the sample C_3F_3-50, in which a diffusion control probably occurs, since an increased activity is observed for a low HHB.

4. Conclusions

The results of the present work accomplished notable progress towards understanding the performance of TPAP encapsulated in fluorinated ORMOSILs (*FluoRuGels*) as catalyst for the oxidation of alcohols in $scCO_2$. We have found that the HHB of the sol–gel matrices is a true structural parameter, dictating reactivity for the oxidative dehydrogenation taking place within the sol–gel cages. The reagents are polar and activity increases with increasing HHB. Indeed, for reactions in $scCO_2$ within very hydrophobic matrices, diffusion is a very fast process and the reaction becomes the controlling step. In this case, the determining interactions are reagents-matrix at the pores' surface (the sol–gel cages).[21]

These findings are important as they show how the materials chemistry, *i.e.* structure and surface properties, dictates the reactivity of catalysts encapsulated in nanostructured sol–gel materials. As a number of sol–gel entrapped catalysts are rapidly finding practical applications in fine chemistry,[22] namely the production of extra pure chemicals in $scCO_2$, the results of the present study provide a general insight that will be useful in guiding the preparation of second generation sol–gel catalysts, including sol–gel entrapped enzymes.

Acknowledgements

This article is dedicated to University of Nice's Professor Jean-Marc Lévy-Leblond in memory of his splendid talk on "Science and Culture" at the 4th Seminar "Marcello Carapezza" (Palermo, March 26, 2007). This work was partially funded by Fundação para a Ciência e a Tecnologia–Project POCTI/QUI/60918/2004. A. Fidalgo acknowledges FCT for post-doc grant SFRH/BPD/20234/2004. CQFM authors acknowledge IN.

References

1 E. Cao, W. B. Motherwell and A. Gavriilidis, *Chem. Eng. Technol.*, 2006, **29**(11), 1372.
2 B. Hinzen and S. V. Ley, *J. Chem. Soc., Perkin Trans. 1*, 1997, **1**, 1907.
3 A. Bleloch, B. F. G. Johnson, V. L. Steven, A. J. Price, D. S. Shephard and A. W. Thomas, *Chem. Commun.*, 1999, 1907.
4 M. Pagliaro and R. Ciriminna, *Tetrahedron Lett.*, 2001, **42**, 4511.
5 R. Ciriminna, S. Campestrini and M. Pagliaro, *Adv. Synth. Catal.*, 2004, **346**, 231.
6 While both homogeneous TPAP and also ORMOSIL-entrapped TPAP show the typical perruthenate-mediated oxidation kinetics consisting of a fast initial stage up to 40–50% conversions, followed by a slower oxidation stage mediated by less reactive RuO_2, the reaction mediated by *FluoRuGel* shows an initial

induction stage followed by a faster linear stage up to complete conversion of the substrate: R. Ciriminna, S. Campestrini and M. Pagliaro, *Org. Biomol. Chem.*, 2006, **4**, 2637.
7 C. Rottman, G. Grader, Y. De Hazan, S. Melchior and D. Avnir, *J. Am. Chem. Soc.*, 1999, **121**, 8533.
8 For example, the dipole moment of the C–F bond in CH_2F_2 is 1.97 Debye. A recent insightful analysis on the biochemical consequences of this enhanced polarity of fluorinated molecules is reported in J. C. Biffinger, H. W. Kim and S. G. DiMagno, *ChemBioChem*, 2004, **5**, 622.
9 B. Ameduri, B. Boutevin, J. J. E. Moreau, H. Moutaabbid and M. Wong Chi Man, *J. Fluorine Chem.*, 2000, **104**, 185.
10 S. V. Ley, J. Norman, W. P. Griffith and S. P. Marsden, *Synthesis*, 1994, 639.
11 R. Ciriminna, S. Campestrini and M. Pagliaro, *Adv. Synth. Catal.*, 2003, **345**, 1261.
12 R. Ciriminna, L. M. Ilharco, A. Fidalgo, S. Campestrini and M. Pagliaro, *Soft Matter*, 2005, **1**, 231.
13 P. Gancitano, R. Ciriminna, M. L. Testa, A. Fidalgo, L. M. Ilharco and M. Pagliaro, *Org. Biomol. Chem.*, 2005, **3**, 2389.
14 A. Fidalgo, R. Ciriminna, L. M. Ilharco and M. Pagliaro, *Chem. Mater.*, 2005, **17**, 6686.
15 L. J. Bellamy, *The Infrared Spectra of Complex Molecules*, Chapman and Hall, N.Y., 3rd edn, 1986, vol. I and II.
16 G. Socrates, *Infrared and Raman Characteristic Group Frequencies*, J. Wiley & Sons, N.Y., 3rd edn, 2001.
17 A. Chmel, E. K. Mazurina and V. S. Shashkin, *J. Non-Cryst. Solids*, 1990, **122**, 285.
18 L. Hench and J. West, *Chem. Rev.*, 1999, **90**, 33.
19 A. Fidalgo and L. M. Ilharco, *Chem.–Eur. J.*, 2004, **10**, 392.
20 A. Fidalgo and L. M. Ilharco, *J. Non-Cryst. Solids*, 2004, **347**, 128.
21 In heterogeneous reactions in $scCO_2$, the CO_2 pressure has great impact on the reaction rate, as density (and thus solvent power) of the supercritical fluid strongly depends on such pressure and because of the interaction between catalyst and CO_2. In general, by careful optimisation it is possible to find temperatures and pressures where the density is in an intermediate range, so the solvent power of the SCF is strong enough to dissolve reasonable amounts of reactants, but the diffusivity is not too much reduced. For a detailed discussion, see: M. S. Schneider, *In situ Phase Behaviour and Infrared Studies of Catalytic Reactions in "Supercritical" Fluids*, PhD thesis, ETH, Zurich, 2004, available at the URL: http://e-collection.ethbib.ethz.ch/ecol-pool/diss/fulltext/eth15424.pdf.
22 R. Ciriminna and M. Pagliaro, *Org. Process Res. Dev.*, 2006, **10**, 320.

